SUPPLEMENTARY INFORMATION

Intratumoral Childhood Vaccine-Specific $CD4^+$ T cell Recall Coordinates Antitumor $CD8^+$ T cells and Eosinophils

Brown, MC et al., 2023

This file contains:
Supplementary Figures 1-13
Supplementary Table 1
Supplementary methods

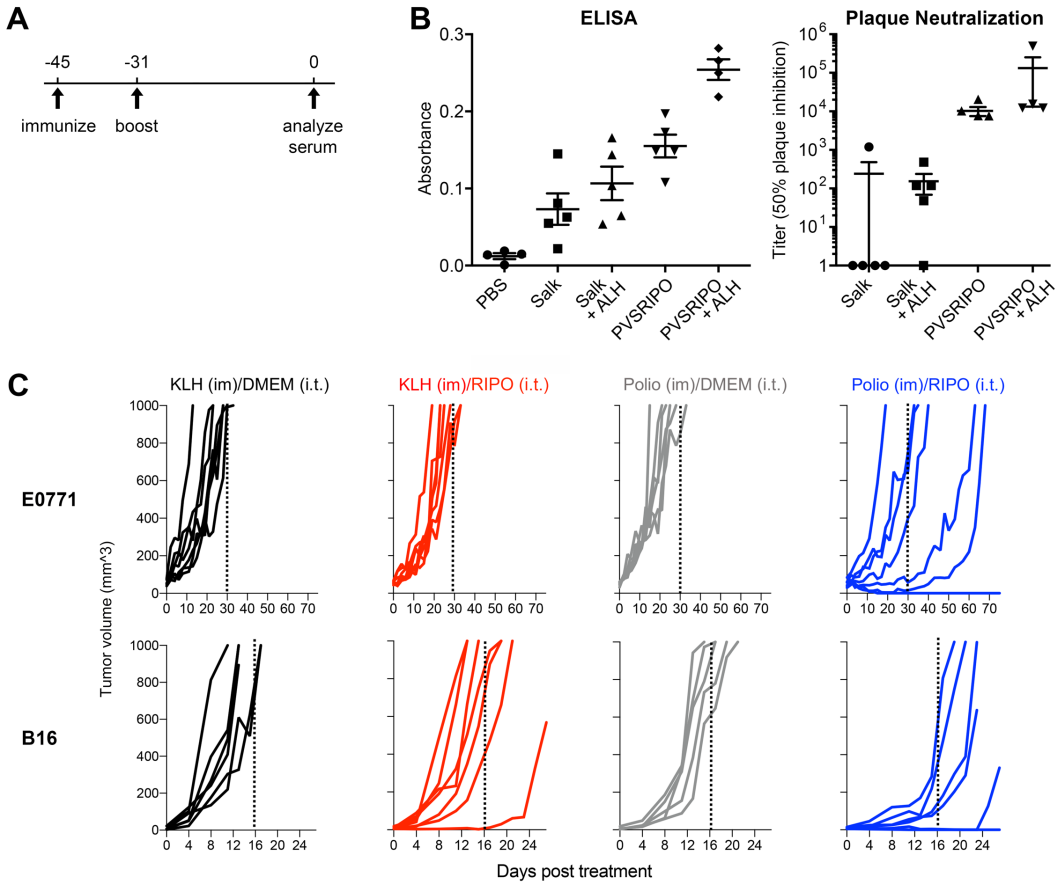

Supplementary Figure 1. (**A**) Schema for immunization validation in (B). (**B**) ELISA (left) and plaque neutralization assay (right) from serum of mice immunized as shown (n= 5/group). (**C**) Individual tumor volumes from experiments shown in Figure 1B.

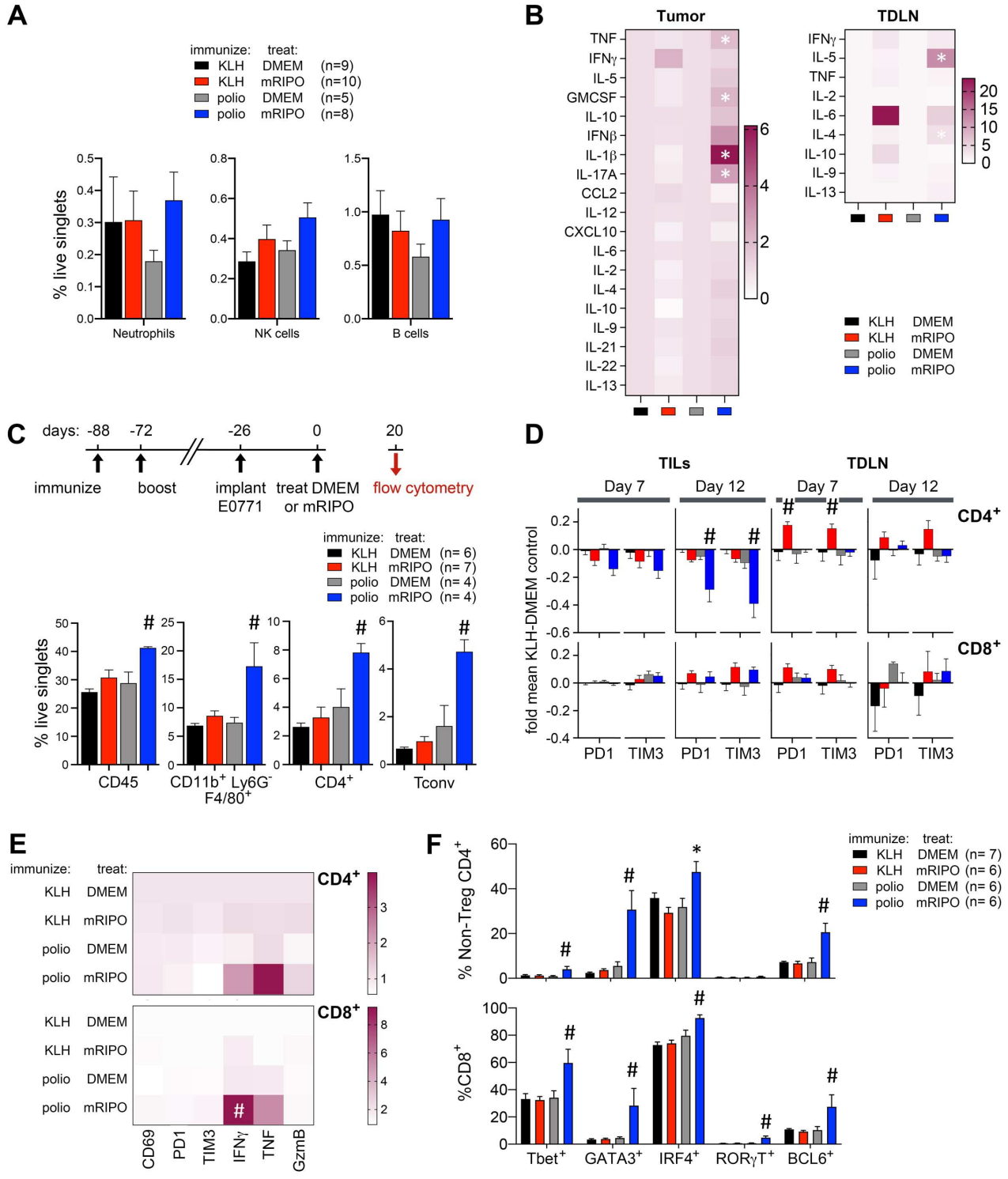
A
immunize: treat:
KLH DMEM (n=9)
KLH mRIPO (n=10)
polio DMEM (n=5)
polio mRIPO (n=8)
% live singlets
Neutrophils
NK cells
B cells
B
Tumor
TDLN
TNF
IFNγ
IL-5
GMCSF
IL-10
IFNβ
IL-1β
IL-17A
CCL2
IL-12
CXCL10
IL-6
IL-2
IL-4
IL-10
IL-9
IL-21
IL-22
IL-13
IFNγ
IL-5
TNF
IL-2
IL-6
IL-4
IL-10
IL-9
IL-13
KLH DMEM
KLH mRIPO
polio DMEM
polio mRIPO
C
days: -88 -72 -26 0 20
immunize
boost
implant E0771
treat DMEM or mRIPO
flow cytometry
immunize: treat:
KLH DMEM (n= 6)
KLH mRIPO (n= 7)
polio DMEM (n= 4)
polio mRIPO (n= 4)
% live singlets
CD45
CD11b+ Ly6G- F4/80+
CD4+
Tconv
D
TILs
TDLN
Day 7
Day 12
Day 7
Day 12
CD4+
CD8+
fold mean KLH-DMEM control
PD1
TIM3
E
immunize: treat:
KLH DMEM
KLH mRIPO
polio DMEM
polio mRIPO
CD4+
CD8+
CD69
PD1
TIM3
IFNγ
TNF
GzmB
F
immunize: treat:
KLH DMEM (n= 7)
KLH mRIPO (n= 6)
polio DMEM (n= 6)
polio mRIPO (n= 6)
% Non-Treg CD4+
%CD8+
Tbet+
GATA3+
IRF4+
RORγT+
BCL6+

Supplementary Figure 2. (**A**) Density of neutrophils, NK cells, and B cells from the experiment presented in Figure 1E. (**B**) (Left) B16 tumor homogenate cytokines 7 days after intratumor mock (DMEM) or mRIPO treatment in KLH or polio immunized mice were measured and normalized to fold respective mean mock control values; asterisks indicate Tukey's post hoc test $p<0.05$ versus mock controls (n=5/group KLH immunized; n=8/group polio immunized). (Right) TDLN cells from KLH or polio immunized B16 tumor bearing mice 7 days after treatment with DMEM or mRIPO were cultured in RPMI 1640+10% FBS for 24 hours and cytokine release was measured (n=2 KLH-DMEM, n=4 for all others); asterisks indicate Kruskal-Wallis post-hoc test $p<0.05$. (**C**) Experimental schema and analyses of infiltrating immune cells in the E0771 model, as done in Figure 1E for the B16 model. (**D**) PD1 and TIM3 surface staining on CD4+ and CD8+ T cells from tumor (TILs) or tumor draining lymph node (TDLN) derived single cell suspensions using the same samples analyzed in Figure 1G-F at day 12 post treatment, values were normalized to log(fold mean KLH-DMEM control). (**E, F**) Analysis of TIL phenotypes in the E0771 model for experiment presented in (C), as done for the B16 model in Fig 1G-F. (**A, C, D, F**) Data bars represent mean + SEM; (**E**) values were normalized as fold mean KLH-DMEM for each marker; (**C-F**) asterisks denote Dunnett's multiple comparison test vs corresponding DMEM treated controls ($p<0.05$, two tailed); # indicates significant Tukey's post-hoc test vs all other groups.

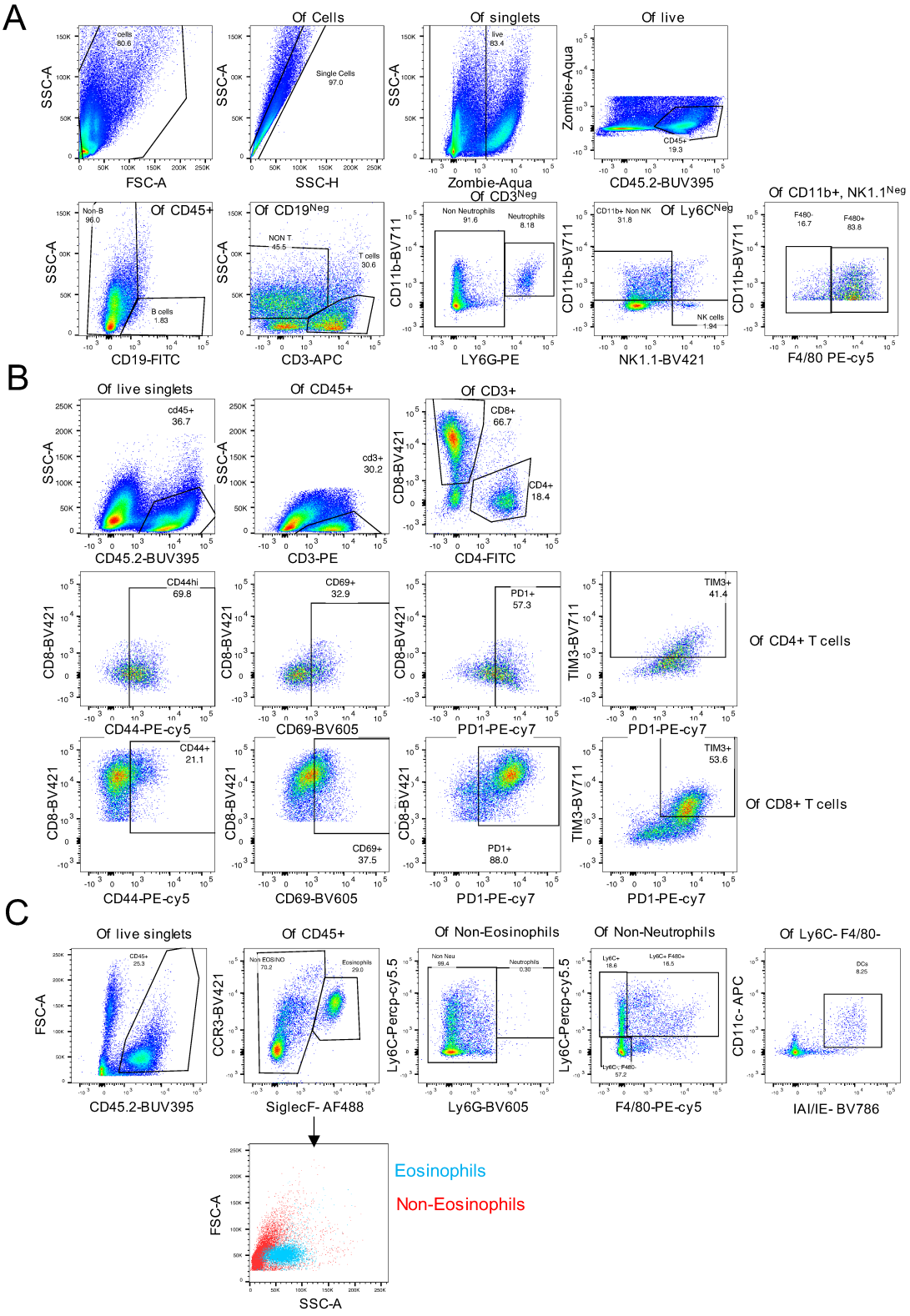
A
Of Cells
Of singlets
Of live
Of CD45+
Of CD19Neg
Of CD3Neg
Of Ly6CNeg
Of CD11b+, NK1.1Neg
B
Of live singlets
Of CD45+
Of CD3+
Of CD4+ T cells
Of CD8+ T cells
C
Of live singlets
Of CD45+
Of Non-Eosinophils
Of Non-Neutrophils
Of Ly6C- F4/80-
Eosinophils
Non-Eosinophils

Supplementary Figure 3. Representative gating strategy for tumor infiltrating cells analyzed in Figures 1E-F and S2. Live singlets were selected after gating of cells, followed by single cells via forward scatter (FSC-A) vs height (FSC-H) comparison, and live/dead using Zombie-Aqua as shown. (**A**) Myeloid cell panel used to gate for B cells, T cells, myeloid cells, and NK cells as shown. (**B**) T cell panel used to gate for $CD4^+$ and $CD8^+$ T cells as well as gating for the indicated antigens on each. (**C**) Eosinophil and myeloid panel to determine the identity of CD11b+ F4/80+ cells identified in Figure 1E: CCR3 and Siglec F were used to gate for eosinophils relative to other myeloid populations and DCs. Confirmation of eosinophil identity was corroborated via confirming their granulocyte identity via SSC-A, and confirming they were $Ly6C^{low/neg}$.

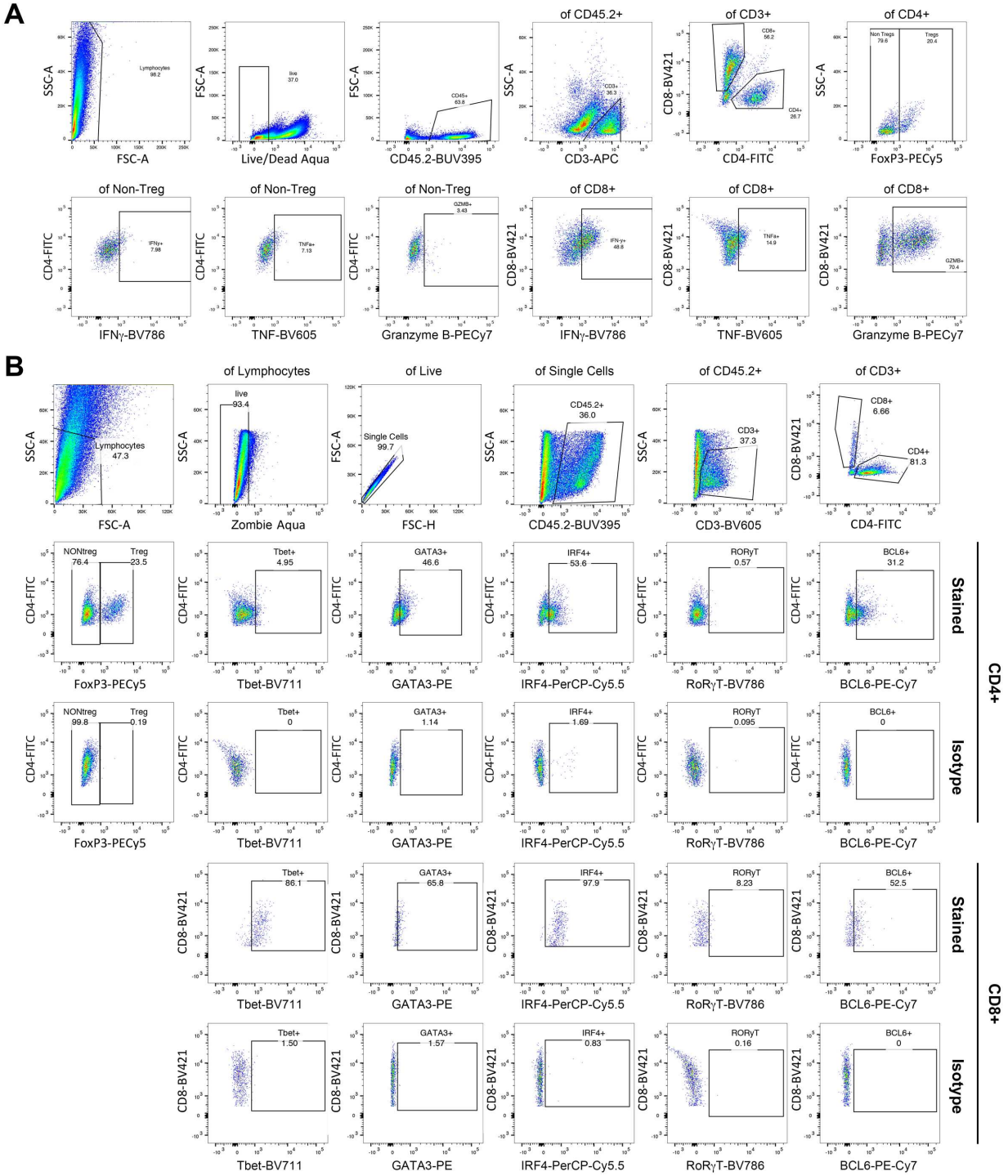
A
of CD45.2+
of CD3+
of CD4+
SSC-A
FSC-A
Lymphocytes 98.2
FSC-A
Live/Dead Aqua
live 37.0
FSC-A
CD45.2-BUV395
CD45+ 63.8
SSC-A
CD3-APC
CD3+ 36.3
CD8-BV421
CD4-FITC
CD8+ 56.2
CD4+ 26.7
SSC-A
FoxP3-PECy5
Non Tregs 79.6
Tregs 20.4
of Non-Treg
of Non-Treg
of Non-Treg
of CD8+
of CD8+
of CD8+
CD4-FITC
IFNγ-BV786
IFNγ+ 7.98
CD4-FITC
TNF-BV605
TNF+ 7.13
CD4-FITC
Granzyme B-PECy7
GZMB+ 3.43
CD8-BV421
IFNγ-BV786
IFN-γ+ 48.8
CD8-BV421
TNF-BV605
TNF+ 14.9
CD8-BV421
Granzyme B-PECy7
GZMB+ 70.4
B
of Lymphocytes
of Live
of Single Cells
of CD45.2+
of CD3+
SSC-A
FSC-A
Lymphocytes 47.3
SSC-A
Zombie Aqua
live 93.4
FSC-A
FSC-H
Single Cells 99.7
SSC-A
CD45.2-BUV395
CD45.2+ 36.0
SSC-A
CD3-BV605
CD3+ 37.3
CD8-BV421
CD4-FITC
CD8+ 6.66
CD4+ 81.3
CD4+
Stained
CD4-FITC
FoxP3-PECy5
NONTreg 76.4
Treg 23.5
CD4-FITC
Tbet-BV711
Tbet+ 4.95
CD4-FITC
GATA3-PE
GATA3+ 46.6
CD4-FITC
IRF4-PerCP-Cy5.5
IRF4+ 53.6
CD4-FITC
RoRγT-BV786
RORγT 0.57
CD4-FITC
BCL6-PE-Cy7
BCL6+ 31.2
CD4+
Isotype
CD4-FITC
FoxP3-PECy5
NONTreg 99.8
Treg 0.19
CD4-FITC
Tbet-BV711
Tbet+ 0
CD4-FITC
GATA3-PE
GATA3+ 1.14
CD4-FITC
IRF4-PerCP-Cy5.5
IRF4+ 1.69
CD4-FITC
RoRγT-BV786
RORγT 0.095
CD4-FITC
BCL6-PE-Cy7
BCL6+ 0
CD8+
Stained
CD8-BV421
Tbet-BV711
Tbet+ 86.1
CD8-BV421
GATA3-PE
GATA3+ 65.8
CD8-BV421
IRF4-PerCP-Cy5.5
IRF4+ 97.9
CD8-BV421
RoRγT-BV786
RORγT 8.23
CD8-BV421
BCL6-PE-Cy7
BCL6+ 52.5
CD8+
Isotype
CD8-BV421
Tbet-BV711
Tbet+ 1.50
CD8-BV421
GATA3-PE
GATA3+ 1.57
CD8-BV421
IRF4-PerCP-Cy5.5
IRF4+ 0.83
CD8-BV421
RoRγT-BV786
RORγT 0.16
CD8-BV421
BCL6-PE-Cy7
BCL6+ 0

Supplementary Figure 4. Representative gating strategy for TIL activation/differentiation status as shown in Figures 1H and S2. Live/dead and singlet discrimination was performed as described in Figure S3. (**A**) T cell panel to determine conventional $CD4^+$ T cell, Treg, and $CD8^+$ densities as well as expression of the indicated intracellular cytokines and granzyme B as shown in Figure 1E and G. (**B**) T cell panel to measure T cell associated transcription factors as shown in Figure 1H; isotype controls for transcription factors were used as shown to guide gating.

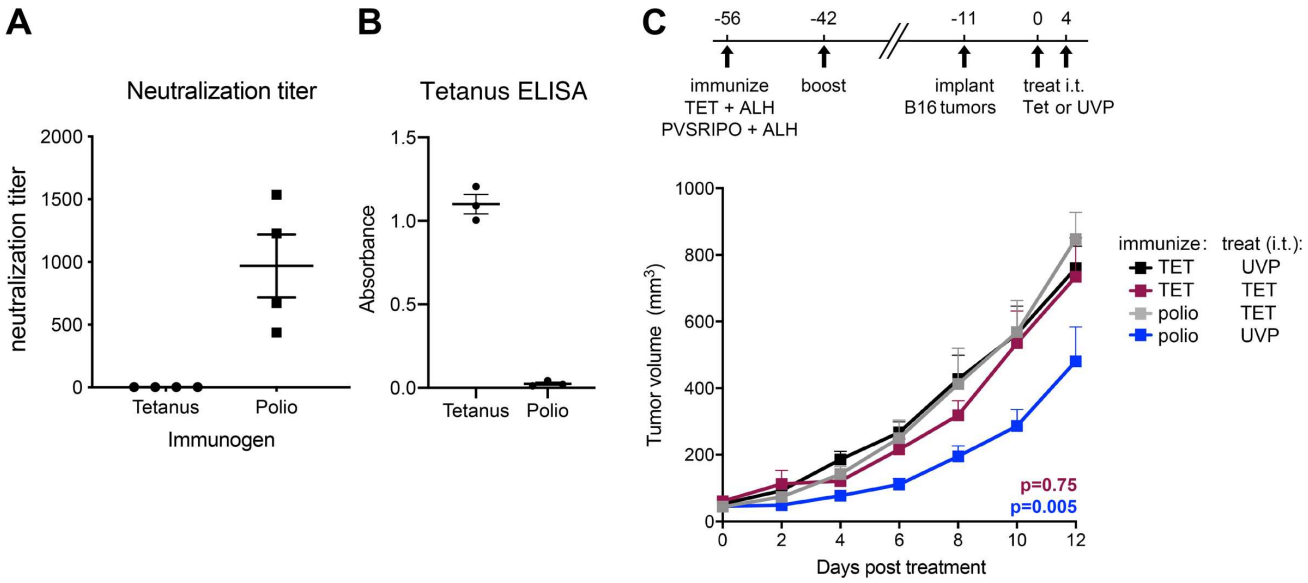

Supplementary Figure 5. (**A, B**) Validation of immunogen-specific serum antibodies for immunization strategies in Figure 2A and B by PVSRIPO plaque neutralization assay (**A**; n= 4/group) and tetanus ELISA (**B**; n= 3/group); mean -/+ SEM is shown. (**C**) Repeat tumor therapy experiment for Figure 2A. Mean tumor volume + SEM are shown (Polio-Tet and Tet-UVP: n= 7; Tet-Tet: n= 6; Polio-UVP: n= 8).

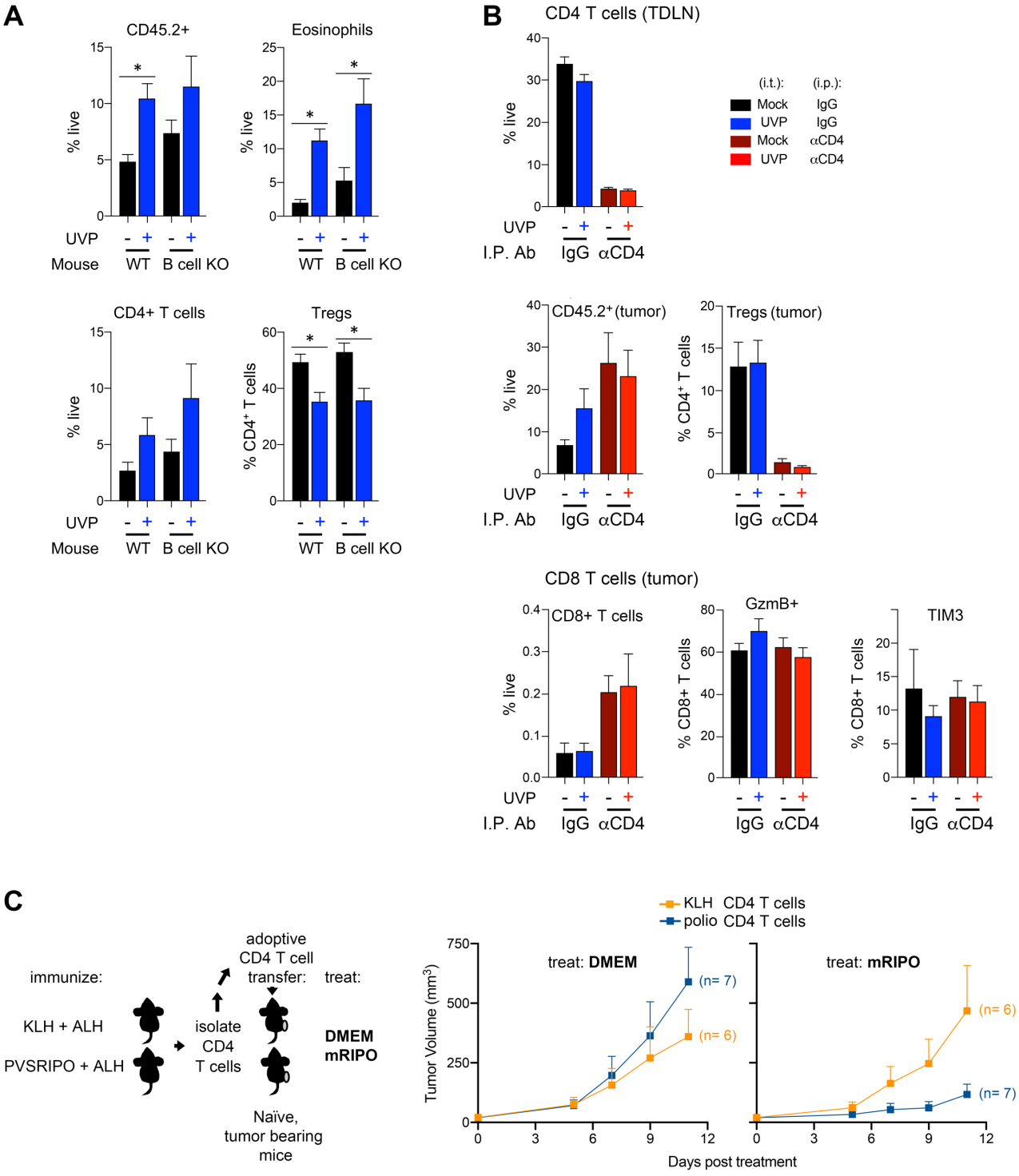
A
CD45.2+
Eosinophils
% live
UVP
Mouse
WT
B cell KO
CD4+ T cells
Tregs
% CD4+ T cells
B
CD4 T cells (TDLN)
(i.t.):
(i.p.):
Mock
IgG
UVP
αCD4
I.P. Ab
CD45.2+ (tumor)
Tregs (tumor)
CD8 T cells (tumor)
CD8+ T cells
GzmB+
TIM3
% CD8+ T cells
C
immunize:
KLH + ALH
PVSRIPO + ALH
isolate CD4 T cells
adoptive CD4 T cell transfer:
treat:
DMEM
mRIPO
Naïve, tumor bearing mice
KLH CD4 T cells
polio CD4 T cells
treat: DMEM
treat: mRIPO
(n= 7)
(n= 6)
Tumor Volume (mm3)
Days post treatment

Supplementary Figure 6. Extended analyses from experiments in Figure 3. (**A**) Flow cytometry analysis of tumors 12 days after mock or UVP from wt or B cell k/o mice immunized and treated as in Figure 3A; mean + SEM is shown; (*) Tukey's post hoc test $p<0.05$. (**B**) Extended flow cytometry analysis of tumors and TDLN from Figure 3D; mean + SEM is shown. (**C**) Tumor volumes from repeat experiment of the assay described in Figure 3E, using $CD4^+$ T cells from KLH or polio immunized mice. Mean tumor volume + SEM are shown.

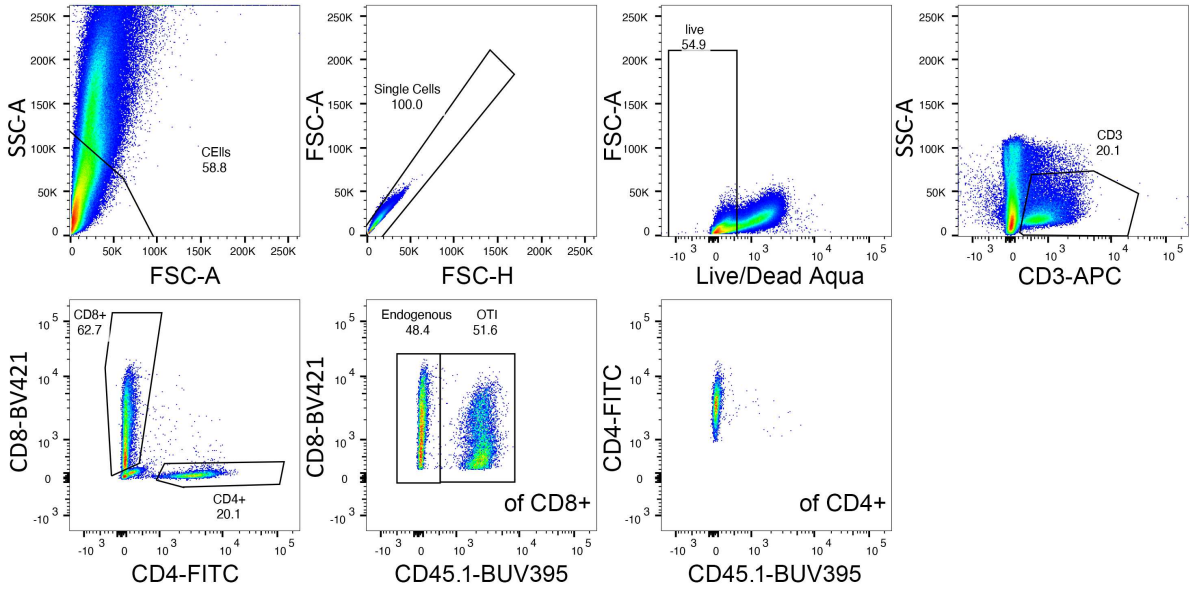

Supplementary Figure 7. Gating strategy for OT-I (CD45.1^{+}) vs endogenous (CD45.1^{Neg}) CD8^{+} T cells in tumors from experiments presented in Figures 4 and S10; gating for markers of activation and differentiation were conducted as shown in Figure S4.

A

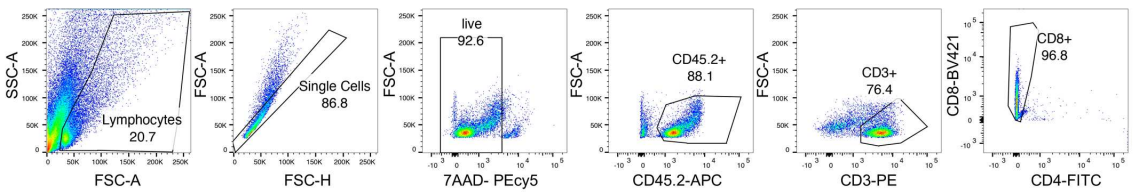

B

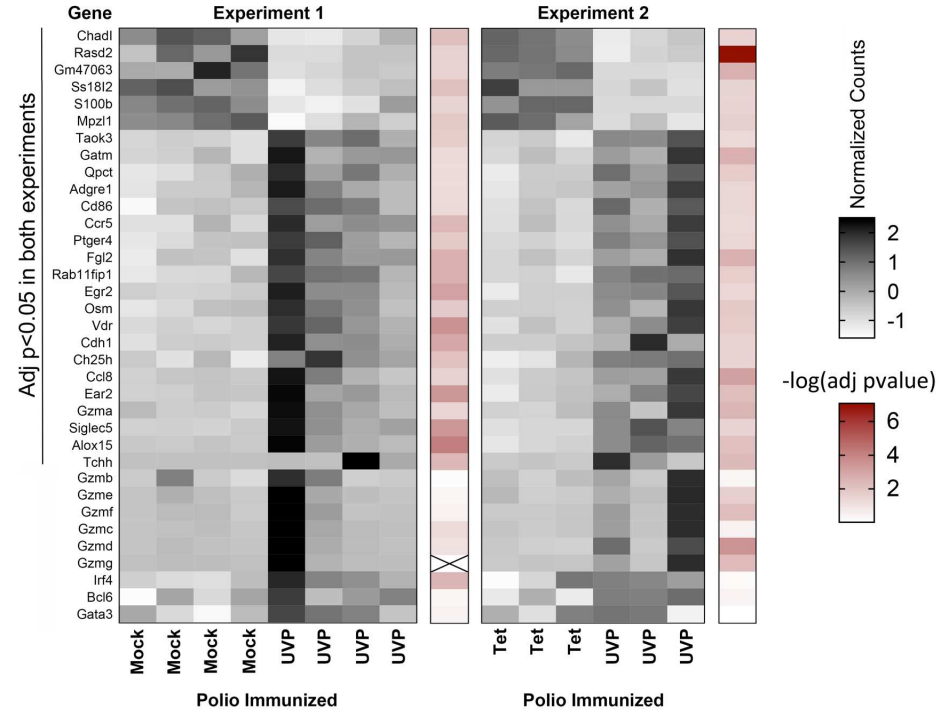

C

Gene name(s)	After UVP	Full name	Relevance	Ref
Chadl	Down	Chondroadherein like	Collogen binding	Uniprot
S100b	Down	S100 calcium binding protein B	expressed in subsets of CTLs, RAGE and NFkb signaling	PMIDs: 19121341, 11705636, 21447379
Gm47063	Down	predicted gene, 47063	Unknown	Uniprot
Rasd2, Viperin	Down	Radical S-Adenyosyl Methionine Domain Containing 2	IFN inducible; Th2 polarization, TCR activation of NFkB and AP-1	PMID: 19047684
Ss18l2	Down	SS18-like protein 2	Unknown	Uniprot
Mpzl1	Down	Myelin Protein Zero Like 1	SRC/SHP2 signaling: SHP2 signaling may suppress antitumor T cell function	PMIDs: 24296779, 33446805, 19290938
Taok3	Up	TAO kinase 3	T cell activation, prevents SHP1 mediated inactivation	PMID: 30373850
Rab11fip1	Up	RAB11 Family Interaacting Protein 1	endosomal recycling, intracellular transport; associated with immune cell influx in cancer	Uniprot; PMID 34764984
Ptger4	Up	Prostaglandin E receptor 4	promotes Th1 differentiation; upregulated on Th17 T cells	PMIDs: 23575689, 29935220
CD86; B7	Up	CD86 molecule	expressed on APCs, Expressed by effector memory T cells	Uniprot; PMID: 9973476
Ccr5	Up	CC motif chemokine receptor 5	chemokine receptor; expressed by activated T cells	PMID: 18632580
Ch25h	Up	cholesterol 25-hydrocylase	produces 25HC; inflammation during viral infection; constrains T cell inflammation in skin	PMIDs: 24994901, 34623903
Osm	Up	oncostatin M	IL6 family, released by T cells, promotes activation of SOCS3, STAT3, STAT5	PMIDs: 17372020, 28093521
Egr2	Up	Early growth response 2	Induce SOCS1/SOCS3 signaling; supports T cell proliferation and homeostasis	PMIDs: 23021953, 25368162
Adgre1; F4/80	Up	Adhesion G Protein-Coupled Receptor E1	cell adhesion, expressed on antiviral CD8 T cells	PMID: 14515257
Vdr	Up	Vitamin D Receptor	T cell development, differentiation, and effector function	PMID: 23785369
Qpct	Up	glutaminyl-peptide cyclotransferase	conversion of N-terminal glutamic acid into pyroglutamine	PMID: 23183267
Fgl2	Up	Fibrinogen-like protein 2	Expressed by CTLs, type I immunity, IRF1 dependent	PMIDs: 3550794, 14976252
Gatm	Up	Glycine amidinotransferase	creatinine biosythesis	Uniprot
Ear2	Up	Eosinophil-associated, ribonuclease A family member 2	eosinophils; cytotoxicity	Uniprot
Alox15	Up	Arachidonate 15-Lipoxygenase	induced by Th2 responses; Fatty acid oxidation; Treg homeostasis	Uniprot, PMIDs: 31333453, 34040168
Siglec5	Up	Sialic acid-binding Ig-like lectin 5	expressed by eosinophils, induced on activated CD8 T cells	Uniprot, PMID: 17272508
Ccl8; MCP2	Up	C-C motif chemokine ligand 8	Skin accumulation of Th2 cells	PMID: 21245898
Gzma	Up	Granzyme A	Cytolysis	Uniprot
Cdh1	Up	cadherein 1	adherence	Uniprot
Tchh	Up	trichohylin	Unknown	Uniprot
Gzmb	Up	Granzyme B	Cytolysis	Uniprot
Gzme	Up	Granzyme E	Cytolysis	Uniprot
Gzmf	Up	Granzyme F	Cytolysis	Uniprot
Gzmc	Up	Granzyme C	Cytolysis	Uniprot
Gzmd	Up	Granzyme D	Cytolysis	Uniprot
Gzmg	Up	Granzyme G	Cytolysis	Uniprot
Irf4	Up	Interferon regulatory factor 4	CD8 T cell effector memory function	Uniprot; PMIDs: 33859042; 24835398
Bcl6	Up	B-cell lymphoma 6	Controls Granzyme expression in CD8 T cells	Uniprot; PMID 17125145
Gata3	Up	GATA Binding Protein 3	type 2 cytokines by CD8 T cells, CD8 T cell homeostasis	Uniprot; PMID 23225883

Supplementary Figure 8. (**A**) Validation of CD45.1+ OT-I+ enrichment after positive CD45.1 selection using tumor suspensions in experiments in Fig 4C; note that OT-I T cells are positive for both CD45.2 and CD45.1, while endogenous T cells were only CD45.2+. (**B**) Normalized transcript counts (black) and -log(False Discovery Rate adjusted p-value) (red) for genes significantly different between OT-I T cells after polio recall (polio immunized mice treated with UVP) vs Mock or Tet treatment in polio immunized mice in two independent experiments as indicated by annotation in figure. In addition, relevant transcripts with protein changes in flow cytometry analyses (Fig 4C): granzymes, IRF4, BCL6, and GATA3 that approached significance in both studies were included; a p-value for Gzmg was not assigned in experiment 1 due to an outlier. (**C**) Table presents known relevance of genes from (B) to T cell biology (PMID= Pub Med ID) and directionality for change (consistent in both replicates) after treatment with UVP in polio immunized mice from two independent experiments.

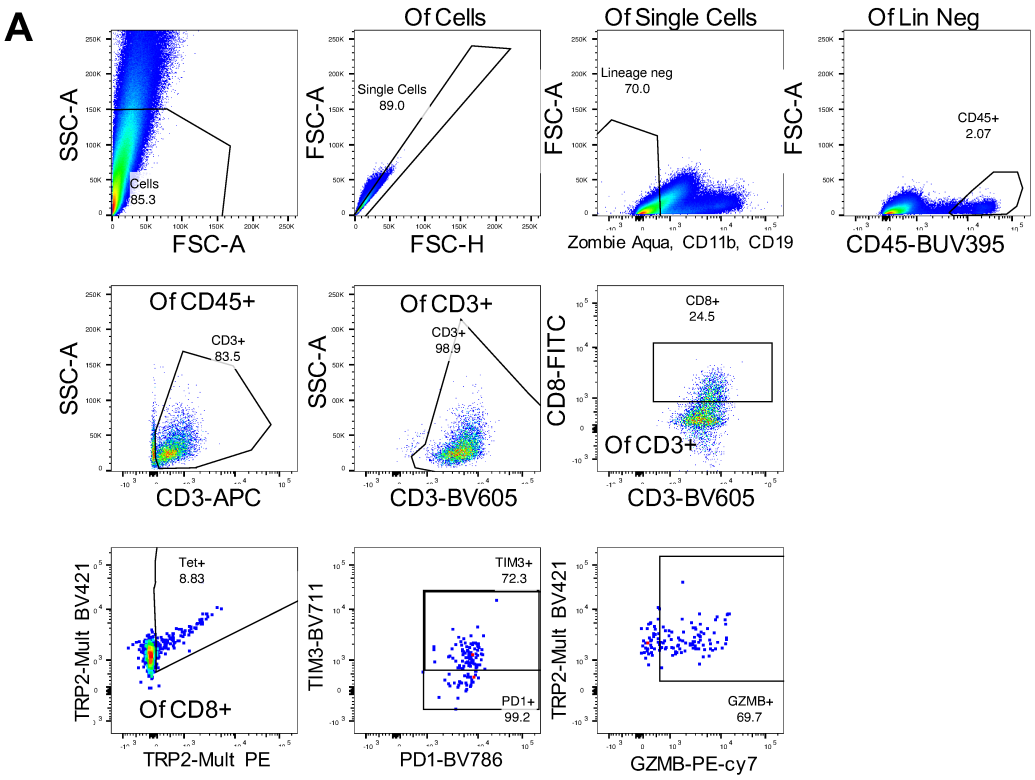
A
Of Cells
Of Single Cells
Of Lin Neg
SSC-A
FSC-A
Cells
85.3
FSC-A
FSC-H
Single Cells
89.0
FSC-A
Zombie Aqua, CD11b, CD19
Lineage neg
70.0
FSC-A
CD45-BUV395
CD45+
2.07
Of CD45+
Of CD3+
SSC-A
CD3-APC
CD3+
83.5
SSC-A
CD3-BV605
CD3+
98.9
CD8-FITC
CD3-BV605
CD8+
24.5
Of CD3+
TRP2-Mult BV421
TRP2-Mult PE
Tet+
8.83
Of CD8+
TIM3-BV711
PD1-BV786
TIM3+
72.3
PD1+
99.2
TRP2-Mult BV421
GZMB-PE-cy7
GZMB+
69.7

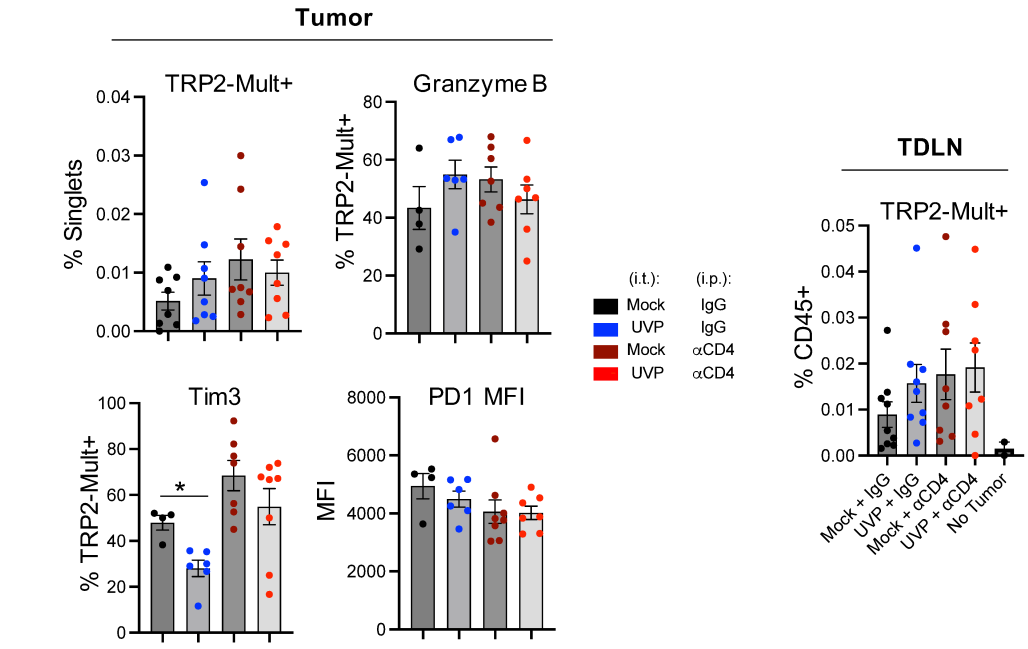
B
Tumor
TRP2-Mult+
% Singlets
Granzyme B
% TRP2-Mult+
Tim3
% TRP2-Mult+
PD1 MFI
MFI
(i.t.):
(i.p.):
Mock
IgG
UVP
IgG
Mock
αCD4
UVP
αCD4
C
TDLN
TRP2-Mult+
% CD45+
Mock + IgG
UVP + IgG
Mock + αCD4
UVP + αCD4
No Tumor

Supplementary Figure 9. TRP2-MHC class I multimer (TRP2-Mult)-specific T cells after polio recall with and without $CD4^+$ T cell depletion. (**A**) Gating strategy for TRP2-MHC-class I multimer (TRP2-Mult) specific TILs in B16 tumors. (**B, C**) Density and phenotype of TRP2-multimer specific $CD8^+$ TILs (B), or percentage of TRP2-multimer specific $CD8^+$ T cells out of CD45+ cells from the TDLN (C). Lymph nodes from non-tumor bearing mice ("No Tumor") were used to confirm specificity of multimer staining. Each data point indicates individual mice; bars and brackets indicate mean -/+ SEM. For phenotypes of TRP2+ T cells, samples with less than 20 TRP2-Multimer+ events were excluded. Note that $CD4^+$ T cell depletion primarily depleted Tregs, which may explain increased levels of TRP2-multimer specific $CD8^+$ T cells in tumors and TDLNs after CD4 T cell depletion (Fig S6).

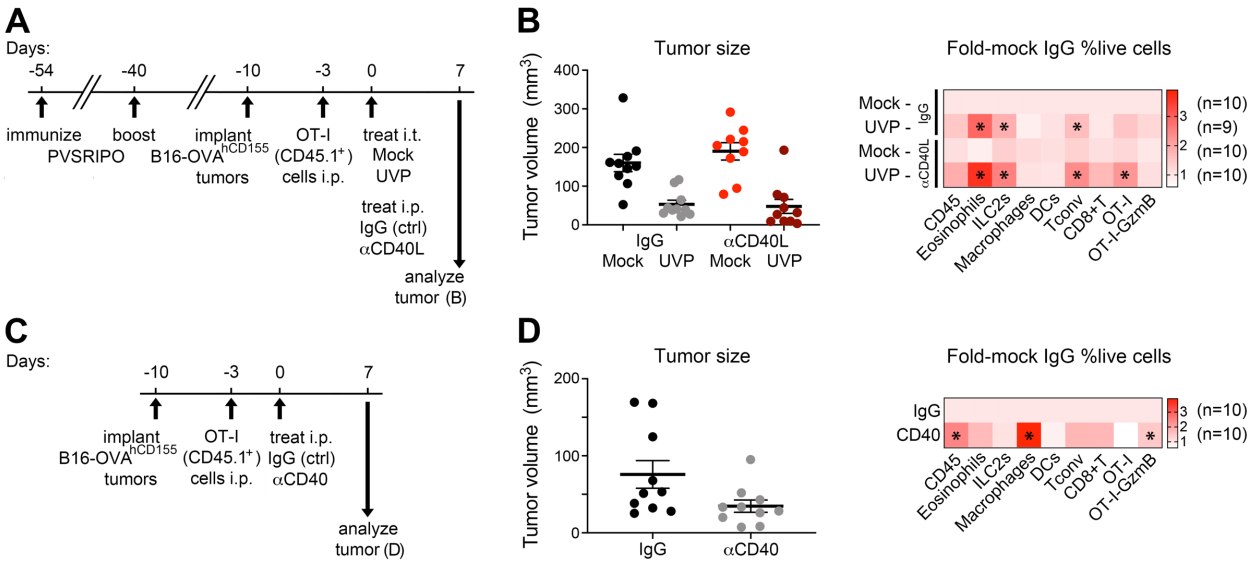

Supplementary Figure 10. The antitumor efficacy of recall antigens is independent of CD40L-CD40 signaling. (**A**) B16-OVA tumor bearing mice previously immunized against polio received adoptive transfer of OT-I T cells followed by intratumor treatment with either mock or UVP concomitant with control IgG or a CD40L blocking antibody (250µg, every 3 days) for experiment shown in (B). (**B**) Tumor volume (left) and analysis of tumor infiltrating immune cells (right) was conducted 7 days after treatment. Data bars depict mean -/+ SEM; heatmap depicts fold-mock IgG control. (**C**) B16-OVA tumor bearing mice received adoptive transfer of OT-I cells followed by intraperitoneal treatment with control IgG or anti-CD40 antibody (50µg/mouse, once) for experiment shown in (D). (**D**) Tumor volume (left) and analysis of tumor infiltrating immune cells (right) were measured 7 days after treatment. Data bars depict mean -/+ SEM; heatmap depicts fold-mock IgG control. Asterisks indicate Dunnett's post-hoc test relative to mock + IgG control (**B**), or unpaired t test relative to IgG control (**D**). All experiments were repeated at least twice and representative series are shown.

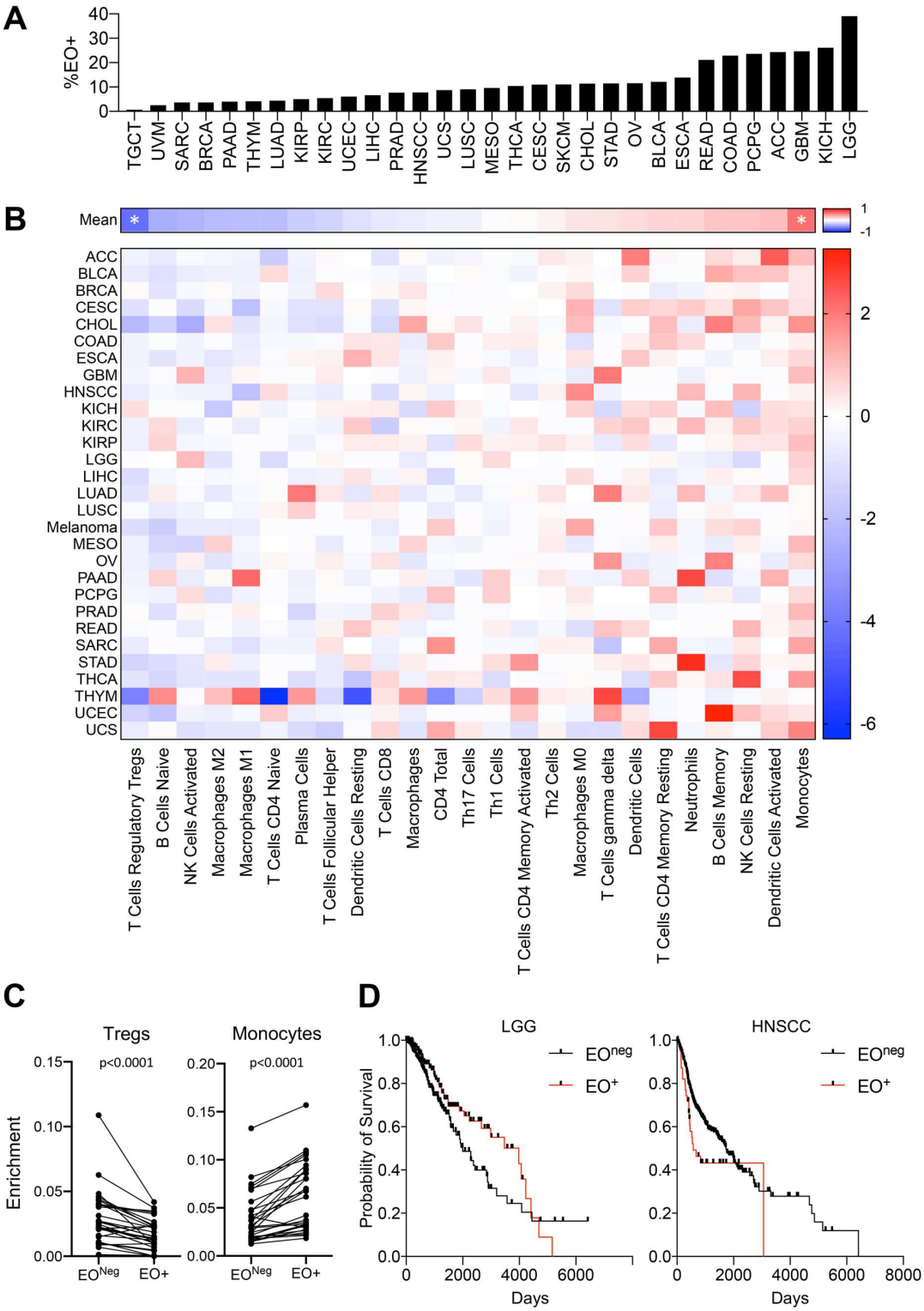
A
%EO+
40
30
20
10
0
TGCT
UVM
SARC
BRCA
PAAD
THYM
LUAD
KIRP
KIRC
UCEC
LIHC
PRAD
HNSCC
UCS
LUSC
MESO
THCA
CESC
SKCM
CHOL
STAD
OV
BLCA
ESCA
READ
COAD
PCPG
ACC
GBM
KICH
LGG
B
Mean
1
-1
ACC
BLCA
BRCA
CESC
CHOL
COAD
ESCA
GBM
HNSCC
KICH
KIRC
KIRP
LGG
LIHC
LUAD
LUSC
Melanoma
MESO
OV
PAAD
PCPG
PRAD
READ
SARC
STAD
THCA
THYM
UCEC
UCS
2
0
-2
-4
-6
T Cells Regulatory Tregs
B Cells Naive
NK Cells Activated
Macrophages M2
Macrophages M1
T Cells CD4 Naive
Plasma Cells
T Cells Follicular Helper
Dendritic Cells Resting
T Cells CD8
Macrophages
CD4 Total
Th17 Cells
Th1 Cells
T Cells CD4 Memory Activated
Th2 Cells
Macrophages M0
T Cells gamma delta
Dendritic Cells
T Cells CD4 Memory Resting
Neutrophils
B Cells Memory
NK Cells Resting
Dendritic Cells Activated
Monocytes
C
Tregs
Monocytes
p<0.0001
p<0.0001
Enrichment
0.15
0.10
0.05
0.00
0.20
0.15
0.10
0.05
0.00
EO^Neg
EO+
EO^Neg
EO+
D
LGG
HNSCC
EO^neg
EO+
Probability of Survival
1.0
0.8
0.6
0.4
0.2
0.0
0
2000
4000
6000
8000
Days

Supplementary Figure 11. Pan-cancer analysis of frequency of eosinophil detection by CIBERSORT within each cancer type (**A**); changes in the frequency of cell types associated with the presence vs absence of detected eosinophils (**B, C**); and survival of LGG and HNSCC by eosinophil detection vs absence corresponding to Figure 5A-B (**D**). (**B**) Asterisks denote significant False Discovery Rate adjusted paired t-test comparing cell type densities across cancer types (n=29); (**C**) p-values are from paired t-test for monocytes and Tregs across cancer types (n=29); (**B, C**) each cancer type was treated as one pair.

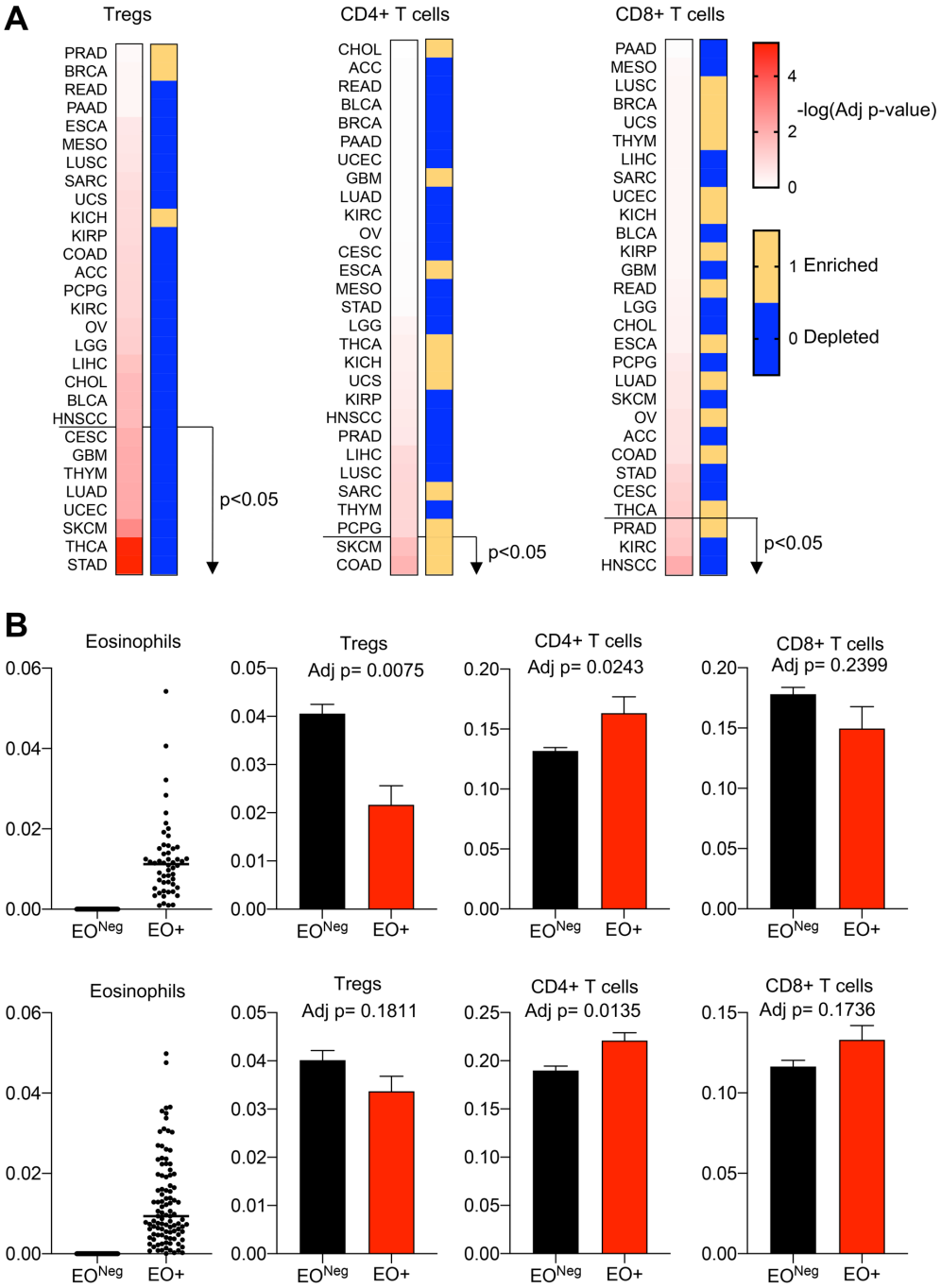
A
Tregs
PRAD
BRCA
READ
PAAD
ESCA
MESO
LUSC
SARC
UCS
KICH
KIRP
COAD
ACC
PCPG
KIRC
OV
LGG
LIHC
CHOL
BLCA
HNSCC
CESC
GBM
THYM
LUAD
UCEC
SKCM
THCA
STAD
p<0.05
CD4+ T cells
CHOL
ACC
READ
BLCA
BRCA
PAAD
UCEC
GBM
LUAD
KIRC
OV
CESC
ESCA
MESO
STAD
LGG
THCA
KICH
UCS
KIRP
HNSCC
PRAD
LIHC
LUSC
SARC
THYM
PCPG
SKCM
COAD
p<0.05
CD8+ T cells
PAAD
MESO
LUSC
BRCA
UCS
THYM
LIHC
SARC
UCEC
KICH
BLCA
KIRP
GBM
READ
LGG
CHOL
ESCA
PCPG
LUAD
SKCM
OV
ACC
COAD
STAD
CESC
THCA
PRAD
KIRC
HNSCC
p<0.05
4
2
0
-log(Adj p-value)
1 Enriched
0 Depleted
B
Eosinophils
Tregs
Adj p= 0.0075
CD4+ T cells
Adj p= 0.0243
CD8+ T cells
Adj p= 0.2399
EONeg
EO+
Eosinophils
Tregs
Adj p= 0.1811
CD4+ T cells
Adj p= 0.0135
CD8+ T cells
Adj p= 0.1736

Supplementary Figure 12. (**A**) Pan-cancer analysis conducted in Fig 5A and Supplementary Figure 11, presenting False Discovery Rate corrected -log(p-value) and directionality (blue= depleted, yellow= enriched) within each cancer type for Tregs, $CD4^+$ T cells, and $CD8^+$ T cells; stratified by p-values (high to low) for difference in Tregs. (**B**) Eosinophil, Treg, $CD4^+$ T cell, and $CD8^+$ T cell predictions for melanoma (SKCM, top) and colorectal cancer (COAD, bottom) for cases with eosinophil detection (EO+) or no eosinophil detection (EO^{Neg}). Adj p-values are from False Discovery Rate corrected paired t-test.

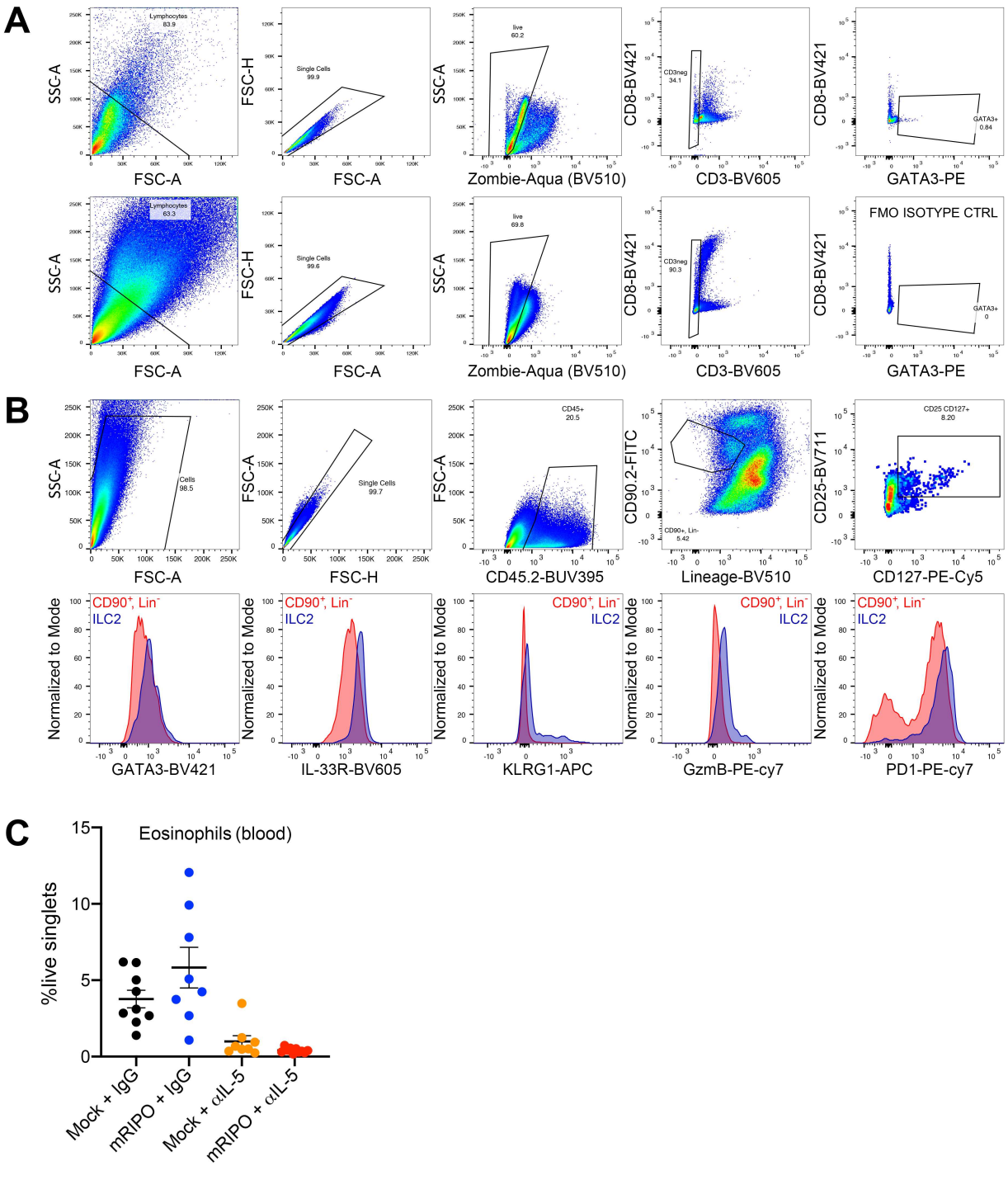
A
SSC-A
FSC-A
Lymphocytes
83.9
FSC-H
Single Cells
99.9
live
60.2
Zombie-Aqua (BV510)
CD8-BV421
CD3-BV605
CD3neg
34.1
GATA3-PE
GATA3+
0.84
Lymphocytes
63.3
Single Cells
99.6
live
69.8
CD3neg
90.3
FMO ISOTYPE CTRL
GATA3+
0
B
Cells
98.5
Single Cells
99.7
CD45+
20.5
CD45.2-BUV395
CD90.2-FITC
Lineage-BV510
CD90+, Lin-
5.42
CD25 CD127+
8.20
CD127-PE-Cy5
CD25-BV711
CD90+, Lin-
ILC2
Normalized to Mode
GATA3-BV421
IL-33R-BV605
KLRG1-APC
GzmB-PE-cy7
PD1-PE-cy7
C
Eosinophils (blood)
%live singlets
Mock + IgG
mRIPO + IgG
Mock + αIL-5
mRIPO + αIL-5

Supplementary Figure 13. (A) Gating strategy for %GATA3+ $CD3^{Neg}$ cells presented in Figure 5C from prior experiments conducted in Figure 4. FMO= florescence minus one. (**B**) Gating strategy for ILC2s in Figures 5G and S10B, D (top), along with representative histograms showing ILC2 vs $Lin^{-}CD90.2^{+}$ cells (bottom). Lineage= Zombie Aqua (live dead), CD3, CD5, CD19, NK1.1, CD11c, CD11b, FCεRIα, γδTCR, αβTCR. (**C**) Blood eosinophil levels determined for the experiment presented in Figure 5D-G.

Supplementary Table 1. Details of antibodies used in this study.

Antigen	Flurophore	Vendor	RRID/Identifier
BCL6	PEcy7	Biolegend	AB_2566196
CCR3	BV421	Biolegend	AB_2565743
CD103	PE	BIolegend	catalog# 156904
CD11b	BV711	Biolegend	AB_2563310
CD11b	BV510	Biolegend	AB_2629529
CD11c	APC	Biolegend	AB_313779
CD11c	BV605	Biolegend	AB_2562415
CD11c	BV510	Biolegend	AB_2562016
CD127	PEcy5	Biolegend	AB_1937261
CD19	FITC	Biolegend	AB_2629813
CD19	BUV395	BD Biosciences	AB_2722495
CD19	BV510	Biolegend	AB_2562137
CD25	BV711	Biolegend	AB_2564130
CD3	APC	Biolegend	AB_2561456
CD3	FITC	Biolegend	AB_312661
CD3	BV510	Biolegend	AB_2562555
CD3	PE	Biolegend	AB_312663
CD4	FITC	Biolegend	AB_312713
CD40	BV605	BD Biosciences	AB_2742809
CD44	PEcy5	Biolegend	AB_312961
CD45.2	BUV395	BD Biosciences	AB_2738867
CD45.2	APCcy7	Biolegend	AB_830789
CD5	BV510	Biolegend	AB_2563930
CD69	BV605	Biolegend	AB_11203710
CD8	BV421	Biolegend	AB_11204079
CD8	FITC	Thermo-Fisher	AB_2538242
CD86	PEcy7	Biolegend	AB_493600
CD90.2	AF488	Biolegend	AB_492886
F4/80	PEcy5	Biolegend	AB_893482
FCgR	BV510	Biolegend	AB_2721324
FoxP3	PEcy5	Thermo-Fisher	AB_468806
GATA3	PE	Biolegend	AB_2562723
Granzyme B	PEcy7	Biolegend	AB_2728381
IA/IE (MHC-II)	BV786	Biolegend	AB_2565977
IFN-g	BV786	Biolegend	AB_2629667
IL33R/ST2	BV605	Biolegend	AB_2860703
IL5	PE	BD Biosciences	AB_395364
IRF4	PercpCy5.5	Biolegend	AB_2728482
KLRG1	APC	Biolegend	AB_10641560
LY6C	PercpCy5.5	Biolegend	AB_1659241
LY6G	PE	Biolegend	AB_1186099
NK1.1	BV421	Biolegend	AB_2562218
NK1.1	BV510	Biolegend	AB_2562217
PD1	PeCy7	Thermo-Fisher	AB_10853805
PD1	BV786	Biolegend	AB_2563680
PDL1	APC	Biolegend	AB_10612741
RORgT	BV786	BD Biosciences	AB_2738916
Siglec F	AF488	Biolegend	catalog# 155524
Tbet	BV711	Biolegend	AB_2715766
TCRb	BV510	Biolegend	AB_2562350
TCRg/d	BV510	Biolegend	AB_2563534
TIM3	BV711	Biolegend	AB_2716208
TNF	BV605	Biolegend	AB_11123912
TruStain FcX	N/A	Biolegend	AB_1574975

SUPPLEMENTARY METHODS:

Polio neutralizing antibody assay and ELISA. Polio neutralization assays were performed as previously described[9]. ELISA to measure anti-polio antibodies was performed using Maxisorp plates (Nunc) coated with $1x10^7$ pfu PVSRIPO; blocked in PBS + 2% BSA + 0.05% Tween-20 (Sigma-Aldrich); incubated with serially diluted sera (1:20, 1:100, 1:500) for 2h; followed by incubation with 1:30,000 protein-A conjugated HRP (Thermo-Fisher) diluted in PBS for 1h; and development using TMB substrate (Thermo-Fisher) followed by blocking the reaction with H2SO4 (Sigma-Aldrich). Absorbance (450nm) was measured using a Tecan Infinite pro plate reader. A similar procedure was used for detection of KLH antibodies and Tetanus-specific antibodies, coating plates at a concentration of 10 or 1μg/ml antigen, respectively.

Tumor homogenate TDLN culture cytokine measurements. Freshly harvested B16 tumors were mechanically homogenized in 1ml PBS. Samples were frozen at -80ºC, thawed, and centrifuged (4,000xG for 10min) to remove solid debris prior to cytokine analysis. Fresh TDLNs (inguinal lymph nodes) were collected in 1ml RPMI-1640 (Gibco), crushed over a 70-micron cell strainer (Olympus Plastics) using a 3ml syringe plunger (BD Biosciences), and resuspended in RPMI-1640 containing 10% FBS. Resulting cell suspensions were plated in a U-bottom 96 well cell culture plate (Greiner Bio-One) at a density of $5x10^6$ and cultured at 37ºC for 24 hours. Cell suspensions were frozen until cytokine measurements were performed. Mouse Anti-Virus and Mouse Th Legendplex kits (Biolegend) were used to determine indicated analyte concentrations per manufacturer instructions, using the manufacturer's analysis software to determine concentration. Cytokines without measurable concentrations above the lower limit of detection for more than 50% of the samples tested were excluded. For samples below the threshold, the threshold value was used.

Adoptive transfer studies and RNA sequencing of tumor infiltrating OT-I T cells. For adoptive transfer of $CD4^+$ T cells from polio or Tet immunized mice, spleens (two each) were harvested. Separately, hCD155-tg C57BL/6 mice were implanted with B16.F10.9^{hCD155} tumors six days prior to splenocyte isolation. Spleens from immunized mice were crushed through a 70μm cell strainer in 3ml RPMI-1640. Resulting cell pellets were reconstituted in 2ml ACK red blood cell lysis buffer (Lonza) and incubated for 10 min at RT, followed by addition of 10ml RPMI and centrifugation.

$CD4^+$ T cells were negatively selected from single cell suspensions using the EasySep™ $CD4^+$ T cell isolation kit (Stemcell Technologies) following the manufacturer's instructions. Two million $CD4^+$ T cells were injected intraperitoneally six days after $B16^{hCD155}$ tumor implantation. Seven days after tumor implantation, recipient mice were treated with mock (DMEM) or mRIPO ($1x10^7$ pfu) and tumor growth was monitored. For adoptive transfer of OT-I x CD45.1 cells, spleens from OT-I x CD45.1 mice were harvested and processed to single cell suspensions as described above. OT-I splenocytes were treated with 10μg/ml SIINFEKL peptide (Invivogen) for 16 hours, washed in PBS, and then $2x10^6$ OT-I splenocytes were transferred in 100μl i.p. For transfer of T cells from mice treated with recall antigen therapy, splenocytes were processed as described above and transferred to naïve recipients immediately following subcutaneous injection of B16.F10.9-OVA cells. For analysis of OT-I T cell transcriptomes after polio recall, mice immunized against polio (PVSRIPO, $1x10^7$ pfu in Alhydrogel) 45 days (prime) and 30 days (boost) prior to B16-OVA tumor implantation received SIINFEKL-activated OT-I splenocytes as described above, and were treated with intratumor mock (PBS) or UVP 9 days after tumor implantation. Twelve days post-treatment tumors were dissociated and subjected to CD45.1 positive selection (MojoSort cell mouse CD45.1 selection kit, Biolegend) per the manufacturer's instructions. A subset of the isolated cells were used to confirm purity by flow cytometry for 7-AAD (Biolegend), CD45.2-BUV395, CD3-PE, CD8-BV421, CD4-FITC; the remaining cells were lysed in 200μl Trizol (Thermo-Fisher). Chloroform extracted RNA from Trizol samples (per manufacturer's instructions) was purified using the RNEasy kit (Qiagen, Inc.) and analyzed on a Hi-seq Illumini sequencer (150bp, PE) at Azenta Life Sciences. Transcripts were aligned with STAR (v2.7) to the GRCm38 mouse genome and differential expression analysis was performed using DESeq2 (v 1.34).

Flow cytometry antibody panels. The panels used in this study include the following antigen-specific antibodies or reagents (see Supplementary Table 1 for antibody sources): lineage panel 1: CD45.2-BUV395 and CD40-BV605, Zombie-Aqua Live/dead, NK1.1-BV421, CD11b-BV711, IA/IE-BV786, CD19-FITC, LY6G-PE, F4/80-PEcy5, CD86-PEcy7, CD3-APC; lineage panel 2: CD19-BUV395, 7-AAD, CD45.2-APC-Cy7, CD11b-BV711, LY6C-PerCP-Cy5.5, LY6G-PE, CD3-FITC, CD11c-APC; lineage panel 3: CD45.2-BUV395 and CD40-BV605, Zombie-Aqua Live/dead, NK1.1-BV421, CD11b-BV711, IA/IE-BV786, CD3/CD19-FITC, LY6G-PE, F4/80-

PEcy7, CD86-PEcy7, CD11c-APC; T cell panel: CD45.2-BUV395, Zombie-Aqua Live/dead, CD3-PE, CD4-FITC, CD8-BV421, CD69-BV605, PD1-PE-Cy7, TIM3-BV711, CD44-PE-Cy5; Intracellular staining T cell panel 1: CD45.2-BUV395, Zombie-Aqua Live/dead, CD3-APC, CD4-FITC, CD8-BV421, FoxP3-PE-Cy5, IFN-γ-BV786, TNF-BV605, Granzyme B-PE-Cy7; intracellular staining T cell panel 2: CD45.2-BUV395, Zombie-Aqua Live/dead, CD3-APC, CD4-FITC, CD8-BV42, FoxP3-PE-Cy5, Tbet-BV711, GATA3-PE, IRF4-PerCP-Cy5.5, RoRγT-BV786, and BCL6-PE-Cy7; OT-I T cell panels were accomplished using the three above T cell panels with exchange of CD45.2 for CD45.1-BUV395; Eosinophil panel: CD45.2-BUV395, CCR3-BV421, Zombie Aqua, CD3/CD19/NK1.1-BV510, CD11c-BV605, CD11b-BV711, IA/IE-BV786, Siglec F-AF488, Ly6C-PERCP-Cy5.5, CD103-PE, F4/80-PECy5, PD1-PEcy7, PD-L1-APC; and ILC2 panel: CD45.2-BUV395, Zombie Aqua, CD3/CD5/CD19/NK1.1/ CD11c/CD11b/FCεRIa/γδTCR/αβTCR-BV510, ST-2(IL33R)-BV605, CD25-BV711, PD1-BV786, CD90.2-AF488, IL5-PE, CD127-PEcy5, Granzyme B-PECy7, KLRG1-APC.

Analysis of TRP2-MHC-class I specific CD8 T cells in B16 tumors and TDLNs. The day before harvest, Flex-T Biotin H2 K(b) TRP2 Monomers (SVYDFFVWL; Biolegend) were multimerized and conjugated with PE or BV421 streptavidin (both Biolegend) according to the manufacturer's instructions. Polio immunized mice bearing B16 tumors treated with mock or UVP in the presence or absence of CD4 depleting antibody (see main text) as described in corresponding figure legends were euthanized; tumors and TDLN (inguinal lymph node) were harvested and dissociated as described in the Materials and Methods section of the main text. After dissociation, single cell suspensions were stained with Zombie Aqua, followed by incubation with the SRC inhibitor Dasatinib (Tocris) in FACs buffer (10% FBS + PBS) at a concentration of 100nM for 30 minutes to prevent TCR internalization during multimer staining. Following incubation, samples were stained for 30min at 4ºC using 2µl per sample of the prepared BV421 and PE bound TRP2-MHCclass I multimers. Surface staining antibodies were then used for staining (see Supplementary Table 1 for antibody information): CD45.2-BUV395, CD19-BV510, CD11b-BV510, CD3-BV605, TIM3-BV711, PD1-BV786, CD8a-FITC, and CD3-APC. Samples were incubated for 30 minutes at 4ºC followed by washing in FACs buffer. Samples were then fixed and permeabilized using the FoxP3/Transcription Factor Staining Buffer Set (Thermo-Fisher), following manufacturer instructions, and stained with Granzyme B-PEcy7 overnight. Cells were washed and

analyzed. Inguinal lymph nodes from non-tumor bearing mice were used to determine TRP2-MHC class I multimer bound $CD8^+$ T cells.

Associations of eosinophils with other cell types in human tumors and survival. CIBERSORT predicted cell type enrichment for each cancer type were obtained from Thorsson et al[37]. Within each cancer type, cases were sorted by eosinophil enrichment, and comparisons were performed between cases with eosinophil score = 0 (EO^{Neg}) vs eosinophil score >0 (EO+). Total $CD4^+$ T cells reflects the sum of the following scores: 'T cells CD4 Memory Activated' + 'T cells CD4 Memory Resting' + 'T cells CD4 Naïve' + 'T cells follicular helper.' For pan-cancer analyses mean enrichment values for each cell type were determined for EO^{Neg} and EO+ for comparison. Mean values from each cell type were scaled and centered within each cell type score across all samples (both EO^{Neg} and EO+), followed by subtracting normalized EO+ from EO^{Neg} values to to generate heatmaps in Fig S9B and Fig S10A. False discovery rate (Benjamini-Hochberg method) was used to adjust for multiple comparisons in Figs S9B and S10A. Hazard ratios and 95% confidence intervals of survival of patients in EO+ vs EO^{Neg} cohorts were determined using the Mantel-Haenszel test and statistical significance was determined using a Mantel-Cox log rank test.